Applied Nanoscience
https://doi.org/10.1007/s13204-023-02857-8

ORIGINAL ARTICLE

Combustion, emission and radiative performance of diffusion flame: effect of graphene nanoparticles

Zohreh Shams[1,2] · Mohammad Moghiman[2] · Mojtaba Baghban[3] · S. H. Pourhoseini[3]

Received: 25 September 2022 / Accepted: 17 April 2023

Abstract
The present work is an experimental study on the effect of graphene NPs on the combustion, emission and radiative characteristics of diesel fuel. The hot plate experiment results show that the ignition probability of the diesel fuel droplets significantly increases in the presence of graphene nanoparticles. By adding graphene NPs, the ignition delay of diesel fuel droplets decreases up to 13%. The fuels were burned in an oil burner subsequently, and flame temperature, luminous and thermal radiation and emissions were measured. The maximum flame temperature increases in the presence of graphene NPs. After the maximum temperature point, the lower temperature of the nanofuel flames compared with pure diesel is due to the higher burning rate of nanofuels. As revealed by the measurements, thermal efficiency increases over the base fuel by 10.1% and 12.7% for the mass fraction of 0.05% and 0.1%, respectively. NO emissions do not change significantly in the presence of graphene NPs. More CO is produced by adding graphene nanoparticles. Also, the addition of graphene NPs considerably increases the radiation heat flux. The thermal and luminous radiation increases by about 7% and 9.67% for diesel fuel containing 0.1% graphene NPs.

Keywords Nonofuel · Ignition probability · Thermal efficiency · Pollutant emission · Luminous radiation · Thermal radiation

Introduction

Due to the growth of energy consumption and the importance of environmental protection, fuel modification has received a great deal of attention. The ignition and combustion properties of liquid fuels can be improved by using additives. Nanofluids have the potential to be used in many areas such as combustion, heat and mass transfer and energy storage, (Keblinski et al. 2005; Choi 2008, 2009; Murshed et al. 2008; Shams et al. 2012). Studies have shown that NP additives positively affect the ignition and combustion features of fuels (Yetter et al. 2009; Chehroudi 2011; Basu and Miglani 2016; Kannaiyan et al. 2017; Aasim et al. 2020). Moreover, conventional systems already in use can operate on nanofuels with little or no changes.

Numerous studies have been done on nanofuels. Some of them have dealt with the behavior of fuel droplets. Gan and Qiao (2011) investigated the combustion behavior of ethanol and decane fuel with Al micro and NPs. They studied the behavior of the fuel droplets through single droplet experiments. They found that the combustion of the fuel droplets containing aluminum NPs, 80 nm in diameter, consisted of five stages: preheating, ignition, classic combustion, microexplosion and surfactant and aluminum ignition. However, the combustion of the fuel containing aluminum microparticles consisted of only the first three stages. The effects of the type of NPs (iron and boron), the concentration of NPs and the type of base fuel (ethanol and decane) on the behavior of nanofuel droplets were investigated by Gan et al. (2012). They found that after the evaporation and complete combustion of the base fuel of a high-concentration nanofuel, if enough energy was released by it, most NPs were ignited as large agglomerates. When the nanofuel was dilute,

✉ Zohreh Shams
shams.z@qiet.ac.ir

✉ Mojtaba Baghban
baghban.mo@gonabad.ac.ir

[1] Department of Energy Engineering, Quchan University of Technology, Quchan, Iran

[2] Department of Mechanical Engineering, Ferdowsi University of Mashhad, Mashhad, Iran

[3] Department of Mechanical Engineering, University of Gonabad, Gonabad, Iran

Published online: 12 May 2023

the base fuel and the NPs combusted simultaneously in the same stage.

The radiation properties of nanofuels have not been adequately investigated. Gan and Qiao conducted two studies on the radiation properties of ethanol containing various NPs (Gan and Qiao 2012a, 2012b). The first study dealt with the effect of aluminum and aluminum oxide NPs on the radiation properties and the evaporation rate of ethanol (Gan and Qiao 2012a). The absorption of radiative energy and hence the evaporation rate were raised considerably by the addition of aluminum NPs, and not as much by the addition of aluminum oxide NPs. In the second study (Gan and Qiao 2012b), the evaporation and radiation properties of ethanol containing carbon NPs and carbon nanotubes were studied. Their results show that NPs raised the evaporation rate of the fuel. The burning rate of ethanol droplets in the presence of aluminum NPs was investigated by Tanvir and Qiao (2014) through droplet stream experiments. They found that higher concentrations of NPs resulted in higher burning rates. Adding 5% (by mass) aluminum NPs raised the burning rate by 140%. Javed et al. (2015) studied the combustion feature and spontaneous ignition of heptane droplets with aluminum NPs at different temperatures. Ooi et al. (2016) used single droplet experiments to investigate the combustion characteristics of diesel containing graphene oxide, aluminum oxide and iron oxide NPs. All three types of NPs improved the fuel combustion properties, while the graphene oxide NPs were the most effective.

Limited studies have used hot plate experiments to explore the ignition properties of nanofuels. Tyagi et al. (2008) studied the effect of adding Al and aluminum oxide NPs to diesel fuel. The ignition probability of the diesel containing NPs was considerably greater than that of the pure diesel. The effect of aluminum oxide, iron oxide NPs and carbon nanotubes on the ignition probability of ethanol was investigated by Huang et al. (2014). They found that the ignition probability of ethanol considerably increases by adding NPs. The increment of ignition probability depends on the concentration and geometry of the NPs. Shams and Moghiman (2017) investigated the effects of the type and size of metal oxide NPs and the droplet size on the ignition characteristic of diesel fuel. In another study, Shams and Moghiman (2018) experimentally studied the effect of metal oxide NPs on the ignition features of diesel fuel. In the presence of metal oxide NPs, the ignition probability significantly increases and the burning time and the ignition zone decrease.

Few studies have been conducted on the performance of nanofuels in furnaces. Mehregan and Moghiman (2014) numerically studied thye combustion properties and pollutant emission of ethanol and decane-containing aluminum NPs. Their results showed that the aluminum NPs reduced the maximum flame temperature and shifted the position of its occurrence downstream the flame. Sungur et al. (2016) recently studied the combustion characteristics and pollutant emission of nanofuels inside a boiler. They found that in the presence of aluminum oxide and titanium oxide NPs, the high temperature zone decreased in size and the thermal efficiency increased by 0.4%. Bazooyar et al. (2018) investigated the effect of adding modified Fe2O3–WO3 particles on the combustion properties and emissions of a semi-industrial boiler. They found that thermal efficiency increases by adding prepared tungsten–ferric FBC.

The radiation behavior of nanofuels in diffusion flames has been the subject of some studies. Waheed et al. (2015) investigated the radiation from the flame of LPG gas and water in the presence of aluminum oxide NPs inside a laboratory furnace. The temperature measurements inside the furnace revealed that the additive aluminum oxide NPs reduced the maximum temperature of the flame and increased the flame radiation. In another study, they investigated the effect of added carbon NPs (Waheed et al. 2014). They found that the addition of carbon NPs reduces radiation in the upstream region of the flame. However, as the NPs moved down the flame axis, they participated in the combustion reactions, which increased the radiation. Boghrati et al. (2017) investigated the effect of adding carbon nanotubes on the radiation flux of the base fuel. They reported that the addition of carbon NPs decreased the flame length and increased the radiation and temperature of the flame. Liu and Liu (2019) used an inverse method to estimate the temperature, concentration fields of soot and metal oxide NPs in asymmetric nanofuel flame.

The addition of NPs to liquid fuels may produce remarkable effects, ranging from improved performance to increased efficiency and decreases in the pollutants emitted from combustion chambers (Afzal et al. 2021). Most studies in this field have dealt with the use of metal and metal oxide NPs (Tyagi et al. 2008; Boghrati et al. 2017; Beloni et al. 2008; Risha et al. 2007; Allen and Lee 2009; Wei et al. 2021; Kaki et al. 2021). However, metal oxide NPs, which are emitted as combustion by-products, may cause pulmonary and respiratory illnesses and skin allergies (Sharifi et al. 2012). Graphene nanolayers, as a type of carbon NPs, have desirable thermophysical and combustion properties.

This study deals with the effect of graphene NPs on the ignition, combustion and radiation properties of diesel fuel and emissions. First, a hot plate experiment is conducted to explore the ignition properties of fuel droplets. Then, the nanofuel containing graphene NPs is subjected to experiments in a furnace to investigate the combustion performance and pollutant emission of the nanofuel flame. Finally, the effect of graphene NPs on luminous and thermal radiations is investigated.

Table 1 The constituent elements and percent composition of diesel fuel

Nitrogen (N)	Sulfur (S)	Hydrogen (H)	Carbon (C)	Component
0.100	0.365	16.200	83.540	Mass fraction (%)

Table 2 The properties of the graphene nanolayers

Nanoparticle	Symbol	Purity	Thickness	Range of particle size
Graphene	G	99.5%	2–18 nm	2–80 nm

Fuel preparation

Diesel is widely used in transportation, agriculture, power generation, aerospace, etc. Because of its many applications, in this study diesel is selected as the base fuel. The specification and percent composition of diesel fuel are given in Table 1.

Graphene has a two-dimensional honeycomb structure of carbon atoms. This gives it a high area-to-volume ratio (Chehroudi 2016). Moreover, compared with metal oxide NPs, graphene nanolayers can participate in combustion reactions and produce less hazardous by-products (Ooi et al. 2016). Due to their desirable properties, graphene nanolayers as thick as 2–18 nm are selected in this study. Table 2 shows the properties of the graphene nanolayers as announced by the manufacturer (Research Nanomaterials, Inc.). The SEM and TEM images of graphene nanolayers are displayed in Fig. 1. To provide a closer look at the size distribution of graphen nanolayers, the images of XRD analysis are shown in Fig. 2.

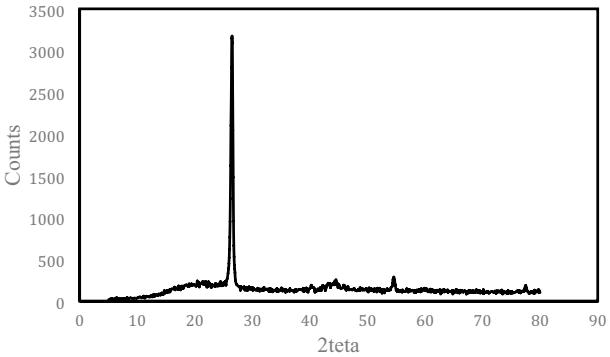

Fig. 2 The result of the XRD processing of the graphene nanolayers. The nanofuel is prepared through two steps. First, NPs are mixed with fuel. Then, the mixture is placed in a UP400-A ultrasonic probe device for 20 min

Experimental setup

Hot plate experiment

The schematic of the hot plate setup is shown in Fig. 3. The experiments were conducted on a 9 cm × 6 cm stainless steel plate heated by ceramic electric elements. A GM900 laser infrared thermometer measured the temperature. The

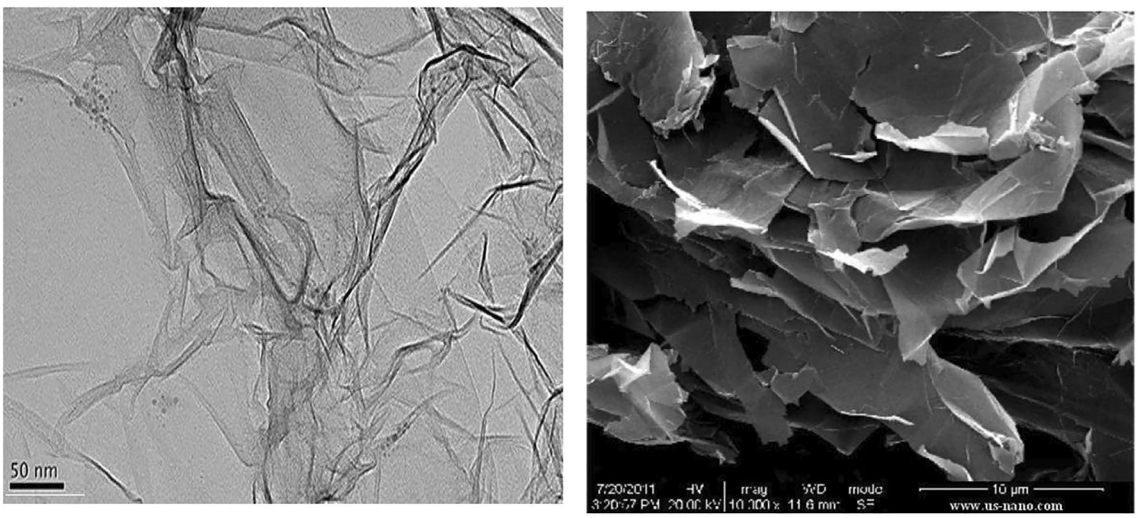

(a) (b)

Fig. 1 **a** The SEM image and b the TEM image of the graphene nanolayers

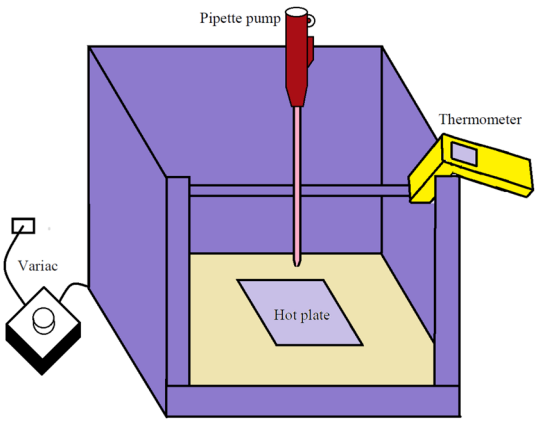

Fig. 3 The image of the hot plate experiments

maximum operating temperature of the thermometer was 900 °C and its accuracy was ± 1.5 °C.

A pipette, 1 ml in volume, was installed over the hot plate. The pipette was positioned at a distance of 2.5 cm from the surface of the hot plate. The average diameter of the fuel droplets was 2.9 mm.

The hot plate experiment started at the plate temperature of 400 °C. The plate temperature was increased by increments of 20 °C at each stage of the experiment until it reached 660 °C. In the beginning, the surface of the plate was cleaned by a very fine 120 grit sandpaper. This removed the material remaining on the surface and reduced its impact on the experimental results. For each of the nanofuels, at each of the plate temperatures, the experiment was conducted on 50 fuel droplets. The experiments were repeated three times to better the accuracy of the results. Throughout the tests, a mechanical stirrer prevented agglomeration and sedimentation of the NPs. The ignition probability at a given temperature was determined by using 50 droplets. Ignition probability is determined as

$$P_{ignition} = \frac{X}{N}, \quad (1)$$

where X is the number of ignited droplets and N is the total number of droplets. Ignition probability is reported as a percent between 0 and 100%. $P_{ignition} = 0\%$ is associated with a low temperature at which no droplet is ignited, while $P_{ignition} = 100\%$ is associated with a high temperature at which all droplets are ignited.

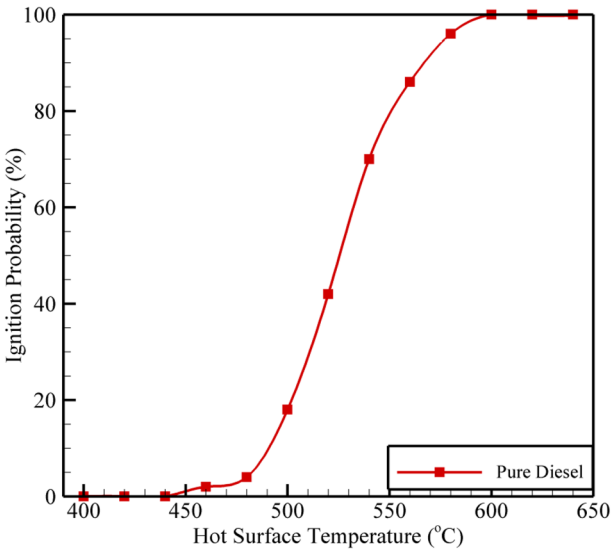

Fig. 5 The ignition probability of pure diesel

Furnace experiment

A laboratory furnace was used to study the combustion process and pollutant emission of the nanofuels (Fig. 4). The combustion chamber was a steel horizontal cylindrical furnace, 1.65 m long and 45 cm in diameter. A layer of mineral wool, which was 50 mm thick, prevented heat loss through the furnace wall.

Along the furnace axis, points at distances of 15, 25, 35, 45 and 55 cm away from the furnace starting section were assigned to temperature measurement. The temperature was measured by type-S thermocouples, with an accuracy of ± 2.5 °C, usable for temperatures up to 1500 °C. The thermocouples were connected to two four-channel TM-947SD data recorders with a sampling rate of 1 s (Fig. 4). For all the nanofuels, the experiments started when the furnace had reached a steady-state temperature. Arrival at a steady state

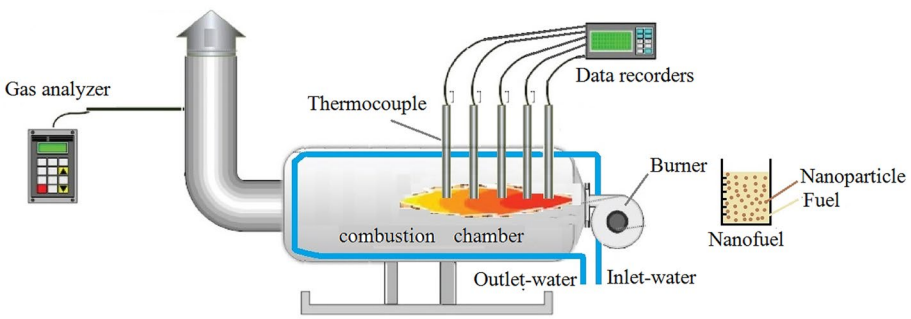

Fig. 4 The configuration of the furnace experiment setup

Table 3 Summary of the experimental studies on hot plate ignition

Fuel	Droplet size	Hot surface material	Ignition temperature range
Diesel (Colwell and Reza 2005)	23.2 µL	304 stainless steel	500 °C–640 °C
Diesel (Shaw et al. 2010)	15.04 µL	409 stainless steel	450 °C–510 °C
Diesel (Shaw et al. 2010)	15.04 µL	stainless steel heat shield	Below 400 °C –560 °C
Diesel (Tyagi et al. 2008)	25.3 mg	Stainless steel	688 °C–768 °C
Diesel + 0.1% Al_2O_3 (50 nm) (Tyagi et al. 2008)	25.3 mg	Stainless steel	Not specified – 748 °C

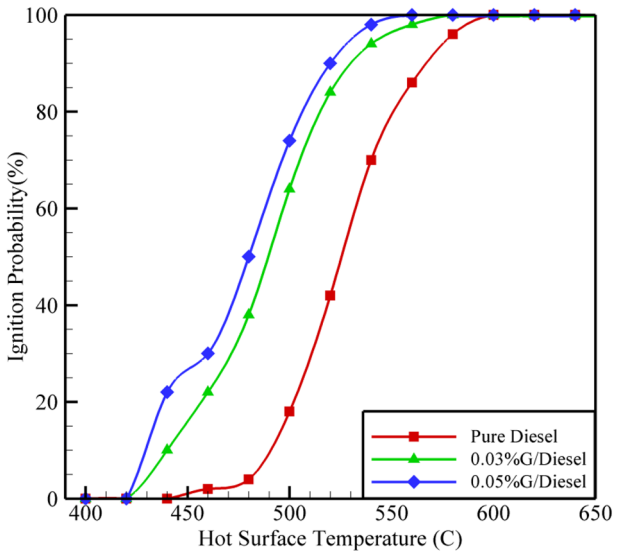

Fig. 6 The ignition probability of diesel containing graphene NPs

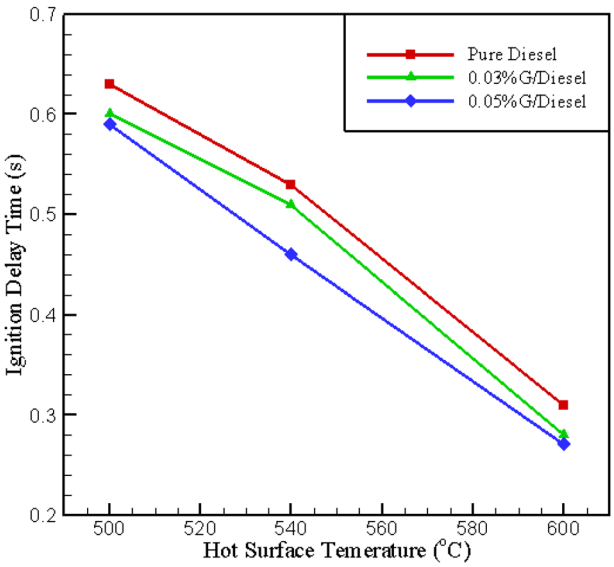

Fig. 7 Ignition delay time (s) (standard uncertainties (u) are u(T) = 4 °C, u(I.D.) = ± 0.04 s)

was indicated by the temperature on the display not changing considerably.

A diesel burner with a maximum capacity of 45,000 kcal/h was used. The fuel system consisted of a pump, an electric valve and a nozzle. The liquid fuel was injected by the pump as very tiny droplets leaving the nozzle. The nozzle was of type AS and was a product of Danfoss. It had a 60° solid cone spray pattern.

The volumetric flow rate of the air was measured by a calibrated flow/velocimeter, Marmonix Man-745 Anemometer, with an accuracy of ± 3%. The average velocity of the incoming air was measured to be 4.62 m/s and the average air flow rate was 122.976 kg/h. The flow rate of the air entering the chamber could be controlled by a damper installed at the air inlet.

To estimate the thermal efficiency, a copper tube was mounted inside the furnace. The water flowed through copper pipes, ½ inch in diameter, which was regularly installed on the inner side of the furnace. The inlet and outlet temperature of water flow were measured by two type-T thermocouples with the maximum operating temperature of 200 °C and the accuracy of ± 0.1 °C. The thermal efficiency of the combustion chamber was calculated by the following relation:

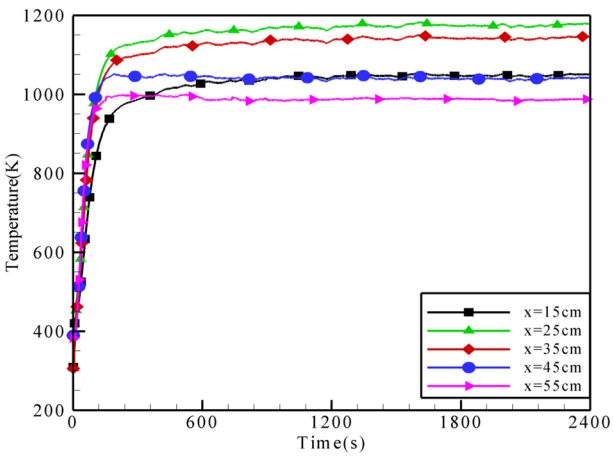

Fig. 8 The temperature variation at five measurement points along the flame centerline

$$\eta_{th} = \frac{\dot{q}_a}{\dot{q}_f} = \frac{\dot{m}_w C_{p,w}\left(T_{out} - T_{in}\right)}{\dot{m}_f LHV}, \quad (2)$$

where $\dot{q}_a$ is the absorption heat by water and $\dot{q}_f$ is the heat released from fuel combustion. $\dot{m}_w$ and $\dot{m}_{fuel}$ denote the flow rate of water and fuel, respectively. $C_{p,w}$ is the specific heat capacity of water. T_{in} and T_{out} are the inlet and outlet temperatures of water. LHV is the lower heating value of the fuel.

A Testo 350 XL gas analyzer was used to measure the degree of pollutant emission. The sampling of the exhaust pollutants was done at a position 1 m below the place where the products exited through the flue into fresh air.

Radiation experiment

A detector was used to measure the infrared and visible radiations, i.e., thermal radiation. Some detectors are sensitive to radiations throughout the entire electromagnetic spectrum, while others accommodate only a partial range of wavelengths. We measured radiations at the visible wavelengths by an SM206 lux meter. It could measure radiations within the visible segment of the electromagnetic spectrum. Its resolution was 0.1 W/m^2 and it was able to measure radiation fluxes up to 3999.9 W/m^2 with an accuracy of ± 5%. Thermal radiation was measured by a thermopile (KIPP & ZONEN, CA-2, 009,574) with an accuracy of 0.016 mV/W/m^2. It can measure radiations at the wavelengths between 0.2 and 50 µm. These wavelengths are responsible for the main part of radiation in combustion (Mehregan and Moghiman 2014). The measurement of radiation flux was carried out outside the combustion chamber in fixed ambient conditions. The thermopile and the lux meter in use were placed at a constant distance from the flame axis. After the heat radiation flux of the flame was measured, the total energy radiated from the flame was calculated by assuming isotropic spherical emission. The result may be stated as the radiative fraction, χ_r:

$$\chi_r = \frac{\dot{q}_r}{\dot{q}_f} = \frac{q\varepsilon 4\pi L^2}{\dot{m}_{fuel} LHV}. \quad (3)$$

In the above relation, q″ is the heat radiation flux and L is the distance between the location of the lux meter and the flame axis. Radiative fraction represents the ratio of the radiation emitted from the flame into the surroundings, $\dot{q}_r$, to the rate of the heat released from the fuel combustion (Waheed et al. 2015).

To get a better insight into the characteristics of the flame, we also took photos of the flame. It was done by a G100EX NEC Avio heat camera, usable between − 40 °C and 1500 °C. It was sensitive to infrared radiations and had an accuracy of ± 2 °C.

Results and discussion

Ignition features

To discuss the effect of graphene NPs on the ignition characteristics, first the behavior of the pure fuel was investigated (Fig. 5). It can be seen that there are low temperatures in which ignition does not occur (ignition probability is 0%) and high temperatures in which ignition always occurs (ignition probability is 100%). For the temperatures between these cases, higher surface temperature meant higher ignition probability. This behavior is similar to those reported by previous studies (Colwell and Reza 2005; Davis et al. 2010). The findings of the other studies and their respective experimental settings are given in Table 3. The difference between previous and present results is attributed to the sensitivity of the hot surface test to the fuel properties and the experimental setting.

Figure 6 shows the ignition probability of diesel fuel droplets containing graphene (G) NPs, at the mass fractions of 0.03% and 0.05%. Results show that the ignition probability increases in the presence of graphene NPs. For instance, the ignition probability at 500 °C, increased from 18 to 56% for diesel containing 0.03% graphene NPs. Also, the ignition probability of the nanofuel increased by increasing the mass fraction of NPs. As the mass fraction of NPs increased from 0.03% to 0.05%, the ignition probability of the nanofuel, at 500 °C and 520 °C, increased by 24% and 15.7%, respectively. It can be seen that the minimum temperature needed for ignition is reduced in the presence of NPs. Further, compared with the pure diesel, the ignition probability of the nanofuels reached 100% at a lower temperature. This result can be explained by a higher evaporation rate and higher burning rate of nanofuel droplet, as compared to pure fuel.

Figure 7 depicts the effect of graphene NPs on the ignition delay. Results show that the ignition delay decreases in the presence of graphene NPs. It can be found that the

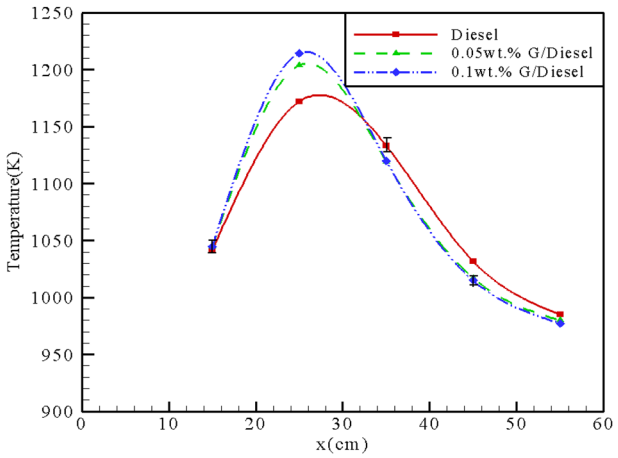

Fig. 9 Temperature distribution in the flame of the diesel fuel and the diesel/graphene nanofuels along the furnace axis

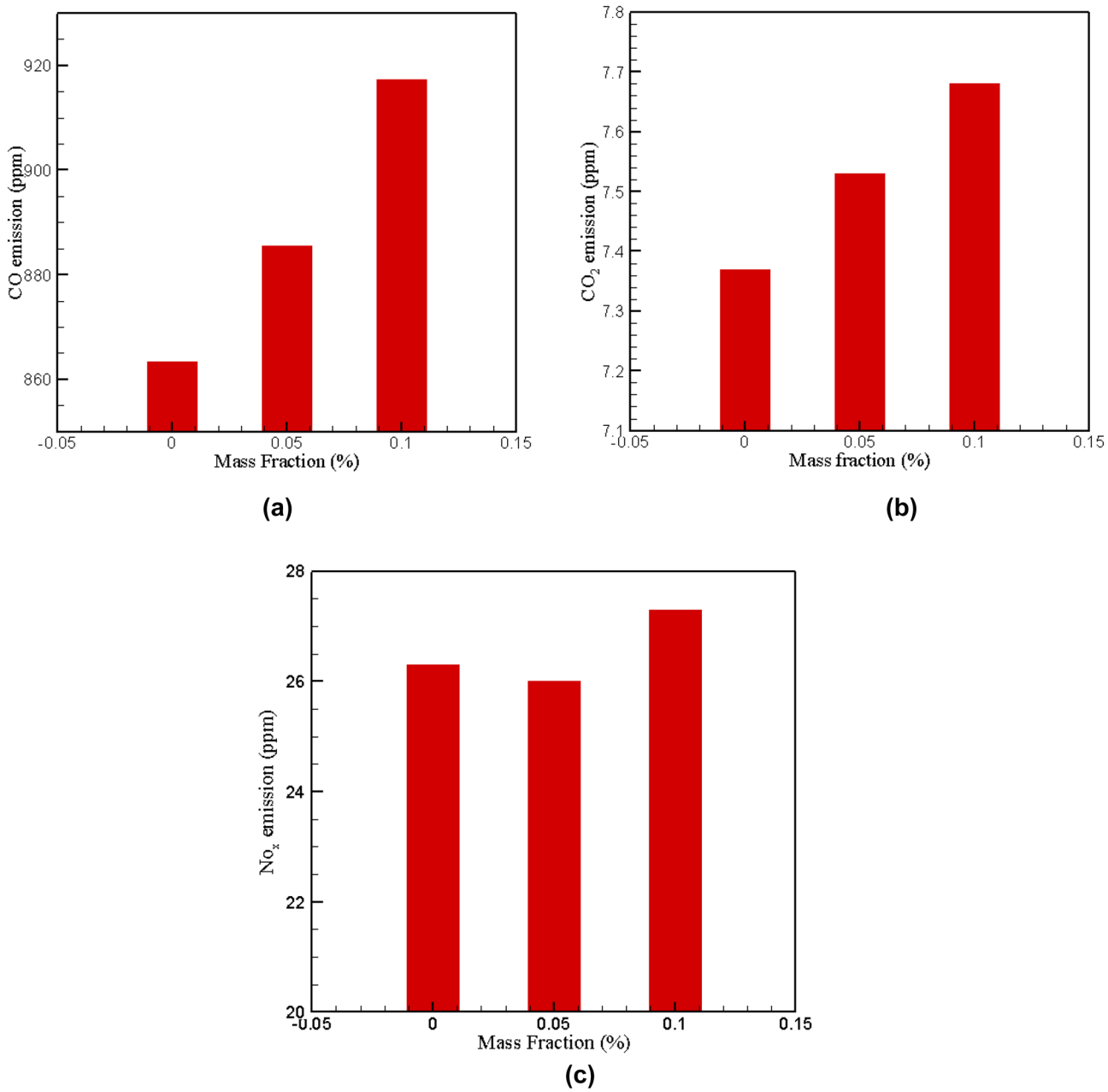

Fig. 10 Effect of graphene NPs on emitted amounts of the pollutants: **a** CO, **b** CO_2 and **c** NO_x emission

addition of graphene NPs decreases the droplet heating time and enhances the evaporation rate. Therefore, the heat and mass transfer rates increase by adding graphene NPs.

Effect of geraphene NPs on combustion features

Based on the elemental analysis, the equivalent molecular formula of diesel fuel can be considered as $C_{16}H_{32}$. In the present study, the fuel/air equivalence ratio is $\varphi = 0.318$. It means that there is a lean-burn combustion with excess air. Figure 8 shows the temperature distributions of pure diesel at the five points inside the furnace for a duration of 40 min since the burner started to operate. As shown, the burner eventually reached a steady state.

Figure 9 shows the temperature distributions along the furnace axis in the steady state. As shown, the added graphene NPs resulted in higher maximum temperatures. Besides, the higher mass fraction resulted in a higher maximum temperature. Graphene NPs are basically made up of

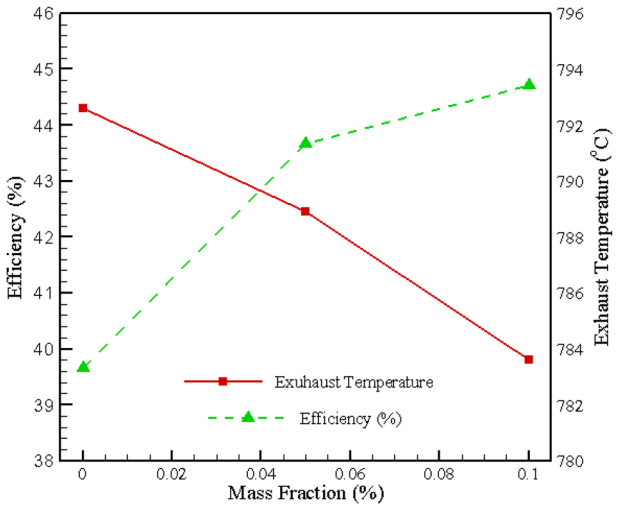

Fig. 11 Effect of graphene NPs on thermal efficiency and exhaust temperature

Table 4 The radiative fraction of diesel

(Dhamale et al. 2011)		(Love et al. 2009)	(Koseki 1989)	Present study
0.27	2700 = Re	0.246	0.35	0.246
0.32	3600 = Re			
0.28	4500 = Re			

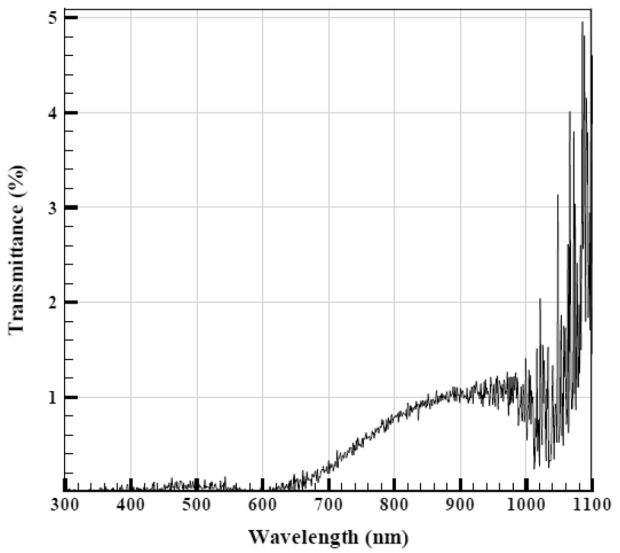

Fig. 12 IR filter transmittance curve

carbon. They tend to have energy-releasing reactions with oxygen, which rises the flame temperature. The lower temperature of the flame of the nanofuels, compared with the diesel fuel, after the maximum temperature point is due to the higher burning rate of the droplets containing NPs. As mentioned for the hot plate experiment, a nanofuel containing graphene NPs has a higher evaporation rate than pure fuel. This causes a quicker combustion of the nanofuel.

The emitted amounts of the pollutants CO, CO_2 and NO_x are presented in Fig. 10. The concentration of CO is presented in Fig. 10a. Results show that the concentration of carbon monoxide increases in the presence of graphene NPs. The amount of carbon monoxide diesel/graphene nanofuels, compared with the base fuel, increases 2.5% and 6.3% for the mass fractions of 0.05% and 0.1%. The reason for the increased concentrations of CO produced by the fuels containing graphene lies in the tendency of graphene to react with oxygen and participate in combustion. Figure 10c presents the effect of graphene NPs on NO_x pollutant emission. Results show that NO_x emission was not affected by adding graphene NPs to diesel fuel.

The flue gas temperature and the thermal efficiency of diesel fuel with and without graphene NPs are presented in Fig. 11. Results show that the exhaust temperature of the furnace decreases in the presence of the graphene NPs, while the presence of the graphene NPs resulted in higher thermal efficiencies. The increases over the base fuel were 10.1% for the mass fraction of 0.05% and 12.7% for the mass fraction of 0.1%.

Finally, the effect of additive graphene NPs on the radiation of flame is discussed. The flames of diesel fuel and nanofuels containing 0.1% (mass fraction) graphene NPs were investigated outside the combustion chamber and in the same ambient conditions. The amount of radiation heat flux depends on the temperature, the emissivity of the gases, and the emissivity of soot. Thermal and luminous radiations were measured by a thermopile and a lux meter, respectively. Also, thermal images produced by the thermal camera were used to find the amount of radiation heat flux along the flame axis. The uncertainties of luminous and thermal radiations were 0.6 W/m^2 and 2.79 W/m^2, respectively.

The thermal radiation from diesel flame was measured to be 86.52 W/m^2. Therefore, the radiative fraction of the diesel was 0.246. The luminous radiation of the diesel was measured by the lux meter to be 4.03 W/m^2. Table 4 includes the radiative fraction of the diesel in this study compared with the results of Koseki (1989), Love et al. (2009), and Dhamale et al. (2011). The differences between this study

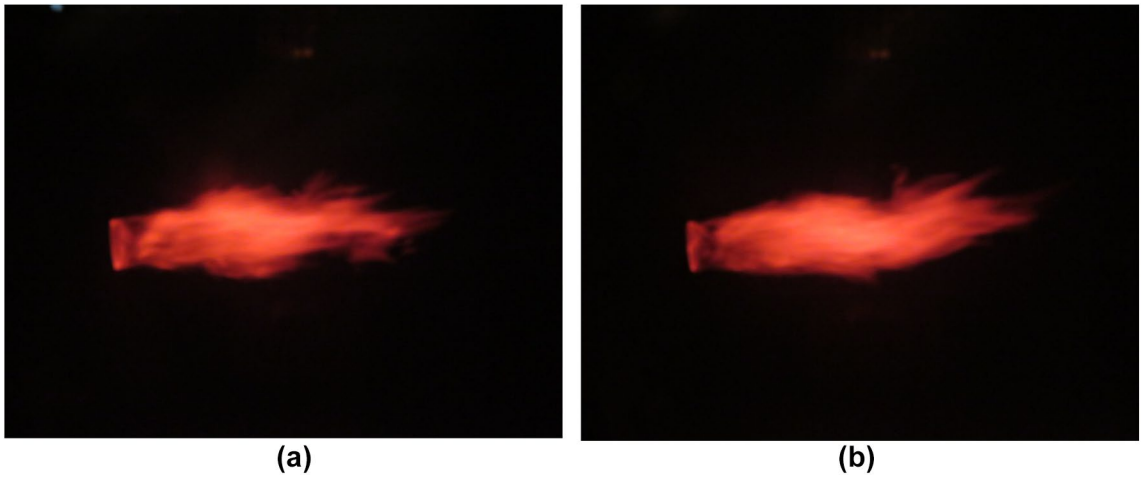

Fig. 13 Flame photograph with filter for: **a** diesel fuel and **b** diesel/graphene nanofuels

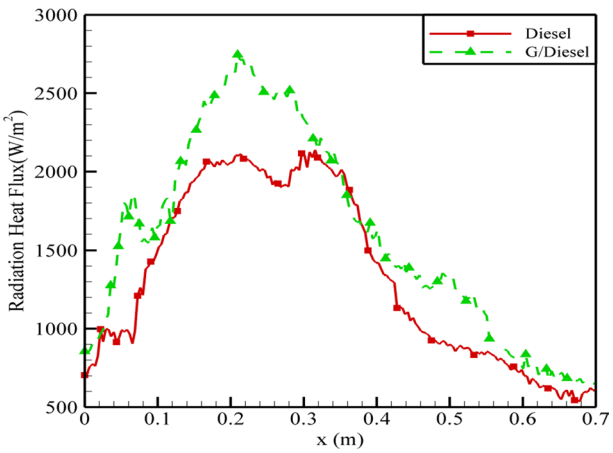

Fig. 14 Distribution of radiation heat fluxes along the axis of the flame of the diesel fuel and the diesel/graphene nanofuel

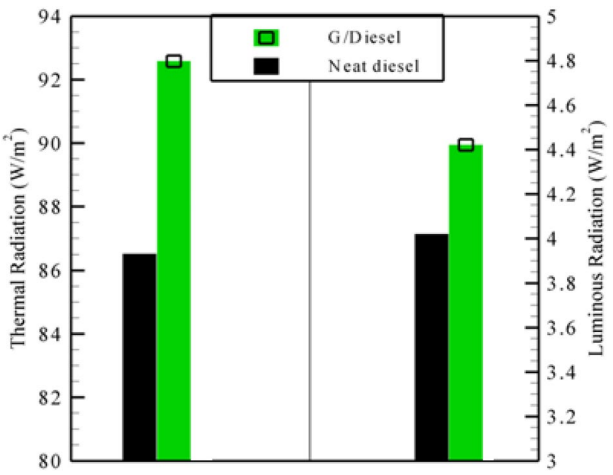

Fig. 15 Thermal radiation and luminous radiation of the flame of the diesel fuel and the diesel/graphene nanofuel

and the previous studies are due to the different compositions of diesel and the experimental settings.

In this paper, the qualitative distribution of soot particles is discussed. The flames were photographed using the filter which only transmits the near-IR wavelengths (Fig. 12) (Pourhoseini and Moghiman 2015). Flame photographs with filter are presented in Fig. 13 for diesel fuel and diesel/graphene nanofuels. It can be seen that adding graphene nanoparticles leads to more soot production which expands the red zone.

The distributions of the radiation heat fluxes along the flame axis for pure diesel and the nanofuel containing the graphene NPs, which were obtained by the thermal camera, are illustrated in Fig. 14. It shows that graphene NPs considerably increases the radiation heat flux. The added graphene NPs raised the maximum value of the radiation heat flux and shifted it upstream the flame. This indicates that the NPs brought about a higher evaporation rate, and hence higher rates of the chemical reactions. Moreover, graphene NPs are made of carbon and participate in combustion reactions, which increases the radiation heat flux of the flame. The findings in this section are confirmed by the hot plate experiment and the furnace experiment.

The presence of graphene NPs inside fuel droplets increases energy absorption. This increases the temperature of the droplets and the evaporation rate of the nanofuel, compared with the base fuel. Previous studies also showed that, when multi-layered carbon nanotubes, at the mass fraction of 0.1%, were added to ethanol fuel, the transmissivity in the visible segment of the electromagnetic spectrum decreased from 90% for the pure fuel to 12% for the nanofuel (Gan and Qiao 2012b). Moreover, the high area-to-volume ratio gives graphene NPs strong reactivity and, being made of carbon, they easily participate in combustion reactions. The released energy is spent on the evaporation of the other

droplets and on the activation of the combustion reactions. Increased evaporation rates, which increase the rates of the chemical reactions of the nanofuel, raise the maximum value of the nanofuel radiation flux and shift the radiation flux upstream the flame.

The thermal radiation from the flame of the diesel containing graphene NPs was measured to be 92.58 W/m^2, which is higher than the one associated with pure diesel. The radiative fraction of the nanofuel containing graphene NPs was 0.263. The luminous radiation of the nanofuel was measured to be 4.42 W/m^2. The presence of the graphene NPs increased the luminous radiation by about 9.67% (Fig. 15).

Conclusion

The effect of graphene NPs on the combustion properties, pollutant emissions and radiation of a diffusion flame of diesel fuel is investigated. The nanofuels were prepared by the addition of graphene NPs, at different mass fractions, to diesel fuel. The main findings are as follows:

The graphene NPs added to diesel fuel considerably increase the ignition probability.

Results show that adding graphene NPs decreases the ignition delay of diesel fuel.

The additive graphene NPs increase the flame temperature in the upstream region, while the nanofuel flame temperature is less than the pure fuel in the downstream.

Compared with the base fuel, the nanofuel containing graphene NPs has a higher thermal efficiency. Thermal efficiency increases over the base fuel 10.1% and 12.7% for the mass fraction of 0.05% and 0.1%, respectively. It means that the same amount of power is generated by consuming less fuel.

The additive NPs do not affect the production of nitrogen oxides in a significant way. They cause more carbon monoxide to be produced.

The results indicate that the thermal and luminous radiations increases about 7% and 9.67%, respectively, in the case of nanofuel compared to that of pure diesel.

Declarations

Conflict of interest On behalf of all authors, the corresponding author states that there is no conflict of interest.

Ethical standard statement The authors declare that for this type of study formal consent is not required.

References

Aasim M, Foto E, Sameeullah M (2020) Nanoparticles for sustainable bioenergy and biofuel production. Biotechnology for Biofuels: a sustainable green energy solution Springer 23–60

Afzal A (2021) Blends of scum oil methyl ester, alcohols, silver nanoparticles and the operating conditions affecting the diesel engine performance and emission: an optimization study using dragon fly algorithm. Appl Nanosci 11(9):2415–2432

Allen C, Lee T (2009) Energetic-nanoparticle enhanced combustion of liquid fuels in a rapid compression machine. In 47th AIAA aerospace sciences meeting including the new horizons forum and aerospace exposition

Basu S, Miglani A (2016) Combustion and heat transfer characteristics of nanofluid fuel droplets: a short review. Int J Heat Mass Transf 96:482–503

Bazooyar B (2018) Mixed modified Fe2O3-WO3 as new fuel borne catalyst (FBC) for biodiesel fuel. Energy 149:438–453

Beloni E, Hoffmann VK, Dreizin EL (2008) Combustion of decane-based slurries with metallic fuel additives. J Propul Power 24(6):1403–1411

Boghrati M, Moghiman M, Pourhoseini SH (2017) The impact of C/H on the radiative and thermal behavior of liquid fuel flames and pollutant emissions. J Braz Soc Mech Sci Eng 39(7):2395–2403

Chehroudi B (2011) Nanotechnology and applied combustion: Use of nanostructured materials for light-activated distributed ignition of fuels with propulsion applications. Recent Pat Space Technol 1(2):107–122

Chehroudi B (2016) Applications of graphene in fuel propellant combustion chehroudi. Propellant Combustion: Graphene Science Handbook 391–398

Choi SU (2008) Nanofluids: a new field of scientific research and innovative applications. Heat Transf Eng https://doi.org/10.1080/01457630701850778

Choi SU (2009) Nanofluids: from vision to reality through research. J Heat Transfer 131(3):033106

Colwell JD, Reza A (2005) Hot surface ignition of automotive and aviation fluids. Fire Technol 41(2):105–123

Davis S, Kelly S, Somandepalli V (2010) Hot surface ignition of performance fuels. Fire Technol 46(2):363–374

Dhamale N, Parthasarathy R, Gollahalli S (2011) Effects of turbulence on the combustion properties of partially premixed flames of canola methyl ester and diesel blends. J Combust 2011:1–13

Gan Y, Qiao L (2011) Combustion characteristics of fuel droplets with addition of nano and micron-sized aluminum particles. Combust Flame 158(2):354–368

Gan Y, Qiao L (2012a) Radiation-enhanced evaporation of ethanol fuel containing suspended metal nanoparticles. Int J Heat Mass Trans 55(21):5777-5782

Gan Y, Qiao L (2012b) Optical properties and radiation-enhanced evaporation of nanofluid fuels containing carbon-based nanostructures. Energy Fuels 26(7):4224-4230

Gan Y, Lim YS, Qiao L (2012) Combustion of nanofluid fuels with the addition of boron and iron particles at dilute and dense concentrations. Combust Flame 159(4):1732–1740

Huang Z (2014) Effect of nanoparticle suspensions on liquid fuel hotplate ignition. J Nanotechnol Eng Med 5(3):031004

Javed I, Baek SW, Waheed K (2015) Autoignition and combustion characteristics of heptane droplets with the addition of

aluminium nanoparticles at elevated temperatures. Combust Flame 162(1):191–206
Kaki S, Kaur BS, Sagari J (2021) Influence of ZnO nanoparticles and dispersant in Baheda oil biodiesel blend on the assessment of performance, combustion, and emissions of VCR diesel engine. Appl Nanosci 11(11):2689–2702
Kannaiyan K, Anoop K, Sadr R (2017) Effect of nanoparticles on the fuel properties and spray performance of aviation turbine fuel. J Energy Resour Technol 139(3):1–8
Keblinski P, Eastman JA, Cahill DG (2005) Nanofluids for thermal transport. Mater Today 8(6):36–44
Koseki H (1989) Combustion properties of large liquid pool fires. Fire Technol 25(3):241–255
Liu G, Liu D (2019) Influence of self-absorption on reconstruction accuracy for temperature and concentration profiles of soot and metal-oxide nanoparticles in asymmetric nanofluid fuel flames. Optik 178:740–751
Love N, Parthasarathy R, Gollahalli S (2009) Rapid characterization of radiation and pollutant emissions of biodiesel and hydrocarbon liquid fuels. J Energy Res Technol 131(1):012202
Mehregan M, Moghiman M (2014) Effect of aluminum nanoparticles on combustion characteristics and pollutants emission of liquid fuels—a numerical study. Fuel 119:57–61
Murshed SMS, Leong KC, Yang C (2008) Thermophysical and electrokinetic properties of nanofluids—a critical review. Appl Therm Eng 28(17–18):2109–2125
Ooi JB (2016) Graphite oxide nanoparticles as diesel fuel additive for cleaner emissions and lower fuel consumption. Energy Fuels 30(2):1341–1353
Pourhoseini S, Moghiman M (2015) Effect of pulverized anthracite coal particles injection on thermal and radiative characteristics of natural gas flame: an experimental study. Fuel 140:44–49
Risha GA (2007) Combustion of nano-aluminum and liquid water. Proc Combust Inst 31(2):2029–2036
Shams Z, Moghiman M (2017) An experimental investigation of ignition probability of diesel fuel droplets with metal oxide nanoparticles. Thermochim Acta 657:79–85
Shams Z, Moghiman M (2018) Effect of metal oxide nanoparticles on the ignition characteristics of diesel fuel droplets: an experimental study. J Braz Soc Mech Sci Eng 40:2–75
Shams Z, Mansouri S, Baghbani M (2012) A proposed model for calculating effective thermal conductivity of nanofluids, effect of nanolayer and nonuniform size of nanoparticles. J Basic Appl Sci Res 2(9):9370–9377
Sharifi S (2012) Toxicity of nanomaterials. Chem Soc Rev 41(6):2323–2343
Shaw A (2010) Evaluation of the ignition of diesel fuels on hot surfaces. Fire Technol 46(2):407–423
Sungur B, Topaloglu B, Ozcan H (2016) Effects of nanoparticle additives to diesel on the combustion performance and emissions of a flame tube boiler. Energy 113:44–51
Tanvir S, Qiao L (2014) Effect of addition of energetic nanoparticles on droplet-burning rate of liquid fuels. J Propul Power 31(1):408–415
Tyagi H (2008) Increased hot-plate ignition probability for nanoparticle-laden diesel fuel. Nano Lett 8(5):1410–1416
Waheed K et al (2014) Investigations on thermal radiative characteristics in a lab scale furnace: effect of addition of nanoparticles to LPG combustion. International Conference on Clean Energy
Waheed K et al (2015) Investigations on thermal radiative characteristics of LPG combustion: effect of alumina nanoparticles addition. Combust Sci Technol 187(6):827–842
Wei J (2021) Comparison in the effects of alumina, ceria and silica nanoparticle additives on the combustion and emission characteristics of a modern methanol-diesel dual-fuel CI engine. Energy Convers Manage 238:114121
Yetter RA, Risha GA, Son SF (2009) Metal particle combustion and nanotechnology. Proc Combust Inst 32(2):1819–1838